MINERALOGICAL CHANGES DURING THERMAL DEMAGNETIZATION OF NATURAL CONTINENTAL SANDSTONES

C. PREZZI[1,2], R. SOMOZA[3] AND R.C. MERCADER[4]

1 Consejo Nacional de Investigaciones Científicas y Técnicas, Instituto de Geofísica D. Valencio, Departamento de Ciencias Geológicas, FCEyN, Universidad de Buenos Aires, Buenos Aires, Argentina (prezzi@gl.fcen.uba.ar)

2 Research Fellow of the Alexander von Humboldt Foundation, Institut für Geowissenschaften, Abteilung Geophysik, Christian Albrechts Universität, Otto Hahn Platz 1, 24118 Kiel, Germany

3 Consejo Nacional de Investigaciones Científicas y Técnicas, Instituto de Geofísica D. Valencio, Departamento de Ciencias Geológicas, FCEyN, Universidad de Buenos Aires, Buenos Aires, Argentina (somoza@gl.fcen.uba.ar)

4 Consejo Nacional de Investigaciones Científicas y Técnicas, Departamento de Física, IFLP, Facultad de Ciencias Exactas, Universidad Nacional de La Plata, Mar del Plata, Argentina (mercader@fisica.unlp.edu.ar)

Received: March 5, 2004; Revised: January 3, 2005; Accepted: January 13, 2005

ABSTRACT

We study the mineralogical changes suffered by specimens of natural miocene red and green continental sandstones (from Pozuelos Formation and Tiomayo Formation) cropping out in the Argentine Puna that increase their bulk magnetic susceptibility and change color when thermally treated. We hypothesize that on heating siderite, which is present in small quantities as cement in the studied sandstones, would oxidize and decompose into maghemite and/or magnetite. Subsequent heating to higher temperatures sometimes would bring about the conversion of maghemite and/or magnetite to hematite. Mössbauer spectroscopy proved to be a very valuable tool for the determination of the presence of siderite in small amounts in the studied samples. The present results show that further work is needed in order to fully understand the mineralogical changes suffered by continental sandstones during heating. The characterization of such changes occurred during laboratory routines is relevant, since they can help to better understand natural processes.

Keywords: siderite, cement, transformation, magnetite, maghemite, hematite

1. INTRODUCTION

Mineralogical changes suffered by natural specimens when subjected to thermal demagnetization have been often reported in paleomagnetic literature. Particularly, many

authors (e.g. *Stephenson, 1967; Schwarz, 1970; Dunlop, 1972; Turner, 1980*) have investigated the rise in the bulk magnetic susceptibility underwent by red and green sandstones when thermally treated, but its causes remain unclear. The characterization of such changes occurred during laboratory routines is relevant, since they can help to better understand natural processes.

In this paper we have studied the mineralogical changes experienced by natural samples of Miocene green and red continental sandstones cropping out in the Argentine Puna. These samples were paleomagnetically studied previously (*Prezzi and Vilas, 1998; Prezzi and Alonso, 2002; Prezzi et al., 2004*) and showed dramatic bulk magnetic susceptibility increases during high-temperature demagnetization in air. Different analyses and experiments were performed. We hypothesize that magnetite and/or maghemite are the transformation products of the high-temperature oxidation of siderite. Other authors have previously studied the magnetic properties of siderite-rich carbonated rocks or of high-purity crystalline siderite (*Ellwood et al., 1986; Zheng et al., unpublished results; Pan et al., 2000; Pan et al., 2002; Frederichs et al., 2003; Isambert et al., 2003*). But the presence of siderite as cement in low quantities, was not previously addressed as one of the possible causes of the rise in the bulk magnetic susceptibility underwent by red and green continental natural sandstones when thermally treated.

The results obtained in this study show that further work is needed in order to fully understand the mineralogical changes suffered by continental sandstones during heating. The examples presented here demonstrate once more the importance that the careful determination of the minerals, that are mainly responsible for the magnetization behavior, has in paleomagnetic studies.

2. CHARACTERIZATION OF SAMPLES

The green continental sandstones and some of the red continental sandstones studied here correspond to Tiomayo Formation (*Seggiaro and Aniel, 1989*). Tiomayo Formation consists mainly of ignimbrites, tuffaceous sandstones, conglomerates, shales and tuffs. Three different sections are identified in Tiomayo Formation: the lower reddish section, the middle yellowish section and the upper greenish section (*Prezzi et al., 2004*). The whole sequence is a thinning- and fining- upward succession, which changes from red conglomerates and sandstones at the base to mostly yellow and greenish mudstones at the top. The upper greenish section crops out in Santa Ana (22°25´S – 66°25´W) and in Morro Blanco (23°00´S – 66°30´W) (Fig. 1). The lower reddish section crops out in Mina Pirquitas (22°40´S – 66°30´W), in Santa Ana and in Morro Blanco (Fig. 1). The reddish section involves a 40 m thick succession of fluviatile conglomerates, sandstones and mudstones that often are interbedded with pyroclastic flow deposits and air - fall tuffs. Two ignimbrites from the base of the section have been dated in 15.7 ± 0.6 Ma (Santa Ana) and 14.9 ± 0.5 Ma (Mina Pirquitas) (*Caffe and Coira, unpublished results*). The upper member of the Tiomayo Formation (70 m thick) is green coloured, and starts with massive sandstones that laterally passes to eolianites showing large-scale cross bedding. The last 40 m of the section are characterized by the presence of biotitic air-fall tuffs and reworked pyroclastic deposits, interbedded with tuffaceous, carbonatic mudstones and lutites (*Prezzi et al., 2004*). The section was formed in a playa lake environment

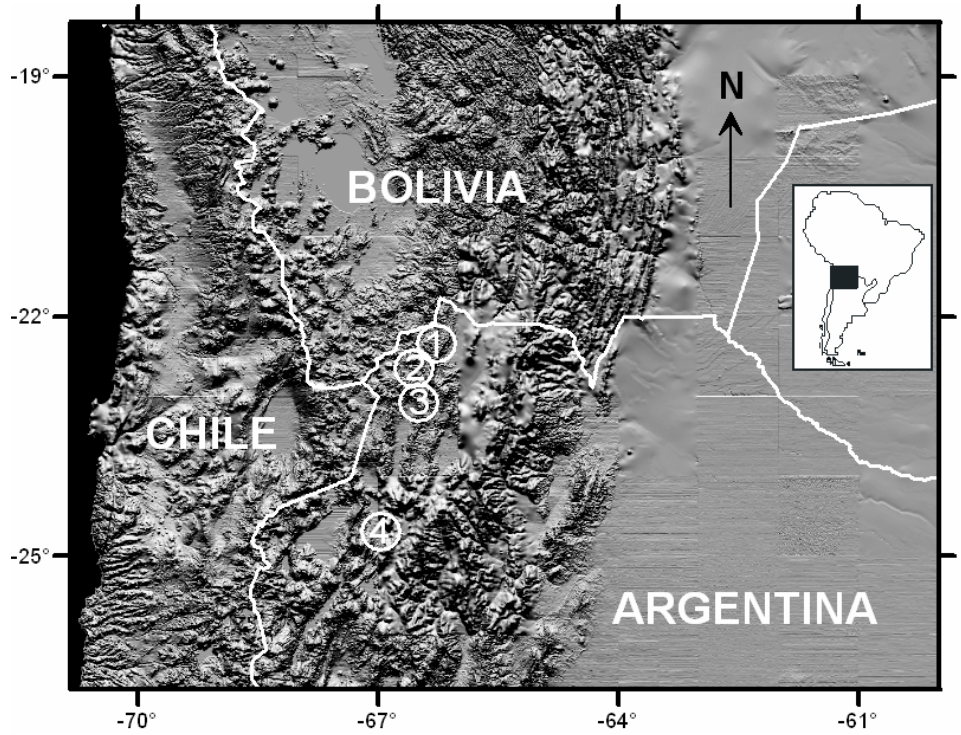

Fig. 1. Topographic map of the Altiplano-Puna showing the localities were the studied samples were collected. 1 - Santa Ana, 2 - Mina Pirquitas, 3 - Morro Blanco, 4 - Bajo de las Siete Curvas.

surrounded by active volcanoes and thermal springs and contains travertine and borates (*Prezzi and Alonso, 2002*). The deposition of the greenish section finished within the middle Miocene, since a tuff from its upper levels in Santa Ana was dated in 12.1 ± 0.5 Ma (*Coira et al., 2005*) (Santa Ana) and an ignimbrite interlayered near the top of the greenish section in Morro Blanco was dated at 10.2 ± 0.3 Ma (*Prezzi and Alonso, 2002*).

The most part of the red continental sandstones studied here correspond to the upper Pozuelos Formation, which crops out in El Bajo de las Siete Curvas (24°40´S – 67°00´W) (Fig. 1). The upper Pozuelos Formation consists mainly of 10–20 cm thick strata of red mudstones with interlaminated gypsum. Fine, medium and coarse sandstones are interlayered along the section. Near the top of the sequence tuffs and tuffaceous sandstones occur. A tuff near the top of the section yielded a hornblende $^{40}Ar/^{39}Ar$ age of 23.8 ± 0.4 Ma (Late Oligocene – Early Miocene) (*Vandervoort, 1993*). The depositional environment was arid continental, probably dominated by playa lakes (*Prezzi and Vilas, 1998*).

The green sandstones showed bulk magnetic susceptibility increases of nearly 150–200% when subjected to demagnetization in air at temperatures between 570–620°C.

Changes in color were also observed during thermal treatment in air: after heating steps of 400–450°C all samples turned yellowish brown in color. Through the observation of thin sections it was determined the existence of moderately rounded to rounded opaque grains. In some samples these grains showed a preferential orientation along thin subparallel layers. These characteristics suggest that the opaque grains are of detrital origin, derived from erosion and reworking. These samples are lithic sandstones with 5–7% quartz, 40% oligoclasic and andesitic plagioclase, 18% andesitic volcanic lithics and 15% glassy clasts. The most important accessory minerals are biotite, green hornblende, lamprobolite and augite (15%), additionally 1–2% of ore minerals are observed. Pores (2–3%) are covered by heulandite/clinoptilolite, which also replaces in part the glassy clasts. The matrix is clayey, greenish in color, probably chloritic (*Prezzi, 1999*). The observation of polished sections allowed to determine that most of the opaque grains are titanomagnetites of nearly 80–120 μm in diameter (Fig. 2A), showing high-temperature oxidation (*Haggerty, 1991*). Ilmeno-hematite trellis lamellae intergrowths along the {111} planes were observed in most titanomagnetite grains. Stages of oxidation range from C1 to C7 (*Haggerty, 1991*). Sandwich and composite oxidation textures were also found. No evidence of low-temperature oxidation (limonitization, maghemitization) was detected. The titanomagnetites observed would correspond to multidomain grain size, but the trellis lamellae divide the grains into isolated smaller magnetic sectors of titano-magnetite poorer in Ti (the Ti being concentrated in the illmenite lamellae).

The red sandstones showed a bulk magnetic susceptibility increase of nearly 200–500% when subjected to demagnetization in air at temperatures between 570–680°C. The clasts of these red samples have plutonic, volcanic and metamorphic origins. The presence of microcrystalline quartz, oligoclasic (An25%) and andesitic (An35%) zonal and not zonal plagioclase, orthoclase, microcline, muscovite, biotite, hornblende, fragments of felsic microcrystalline matrix with spherulitic texture, scarce fragments of phyllites and quartzites and clays (illite) was determined (*Prezzi, 1999*). The existence of hematite as cement was observed. From examinations of polished sections it was determined that (titano)magnetite, hematite, ilmenite, limonite, pyrite and gold are present. Scarce (titano)magnetite crystals of nearly 100 μm in diameter and more

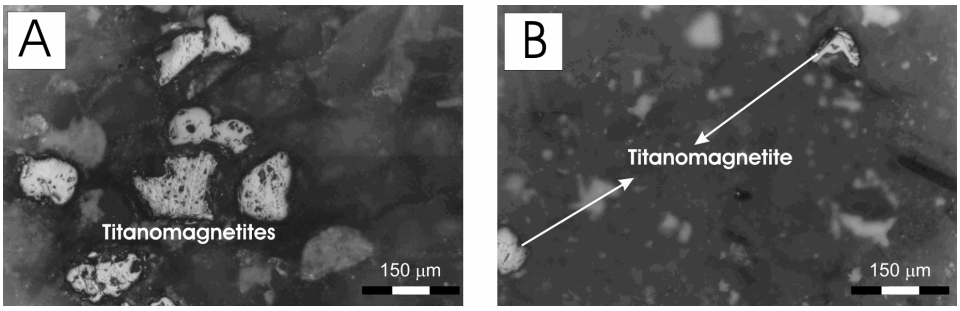

Fig. 2. Microphotographs of microscopy observation. **A** - polished section of a natural green sandstone specimen, where numerous grains of (titano)magnetites can be observed. **B** - polished section of a natural red sandstone specimen showing the presence of (titano)magnetite grains.

numerous ones of 10–30 μm in diameter were observed (Fig. 2B). Such crystals are of detrital origin. It was not possible to determine the Ti content of (titano)magnetite. Hematite was identified as an alteration (limonitization) product. Hematite exsolution textures were observed in detrital ilmenite crystals of nearly 30 μm in diameter. Limonite was recognized as a weathering product. Very scarce pyrite of nearly 10–20 μm in diameter and gold of nearly 5 μm in diameter as inclusions were observed in each polished section.

In the following sections the green continental sandstones' samples corresponding to the greenish section of Tiomayo Formation collected in Santa Ana are labeled BR. The red continental sandstones' samples obtained from the reddish section of Tiomayo Formation in Santa Ana are labeled SA, the ones obtained in Mina Pirquitas are labeled PK. The red continental sandstones' samples from the upper Pozuelos Formation are labeled A.

3. EXPERIMENTAL PROCEDURES AND METHODS

Different analyses and experiments were performed on specimens of the green (BR) and red (SA, PK and A) sandstones that showed the above mentioned bulk magnetic susceptibility increase when subjected to thermal demagnetization.

Thin and polished sections of heated and unheated specimens of BR, SA, PK and A samples were microscopically analyzed by transmitted (magnifications of 2.5, 10, 25 and 40 were used) and reflected light through oil immersion (magnifications of 16 and 50 were used) respectivelly.

Thermomagnetic curves in air were carried out on unheated and heated up to 620°C specimens of BR48 sample. Isothermal remanent magnetization (IRM) acquisition, back field and hysteresis experiments were conducted on natural and on the correspondent thermally demagnetized specimens of different BR, SA, PK and A samples. Bulk magnetic susceptibility (κ) vs. temperature (T) curves were performed in air atmosphere on unheated BR, PK and A samples.

X-ray diffractometry (XRD) was carried out on bulk and on the clay fraction (< 2 μm) of 550°C heated and unheated specimens of sample BR48. XRD data were obtained in a Philips 1130 diffractometer with CuKα radiation (filtered with Ni), at 40 kV, 20 mA, swept at 2°/min and 1°/cm, in the range $10 < 2\Theta < 130°$.

Quali- and quantitative chemical analyses were carried out on unheated and heated up to 600°C specimens of the BR48 sample. Quantitative chemical analyses were performed on unheated and heated up to 700°C specimens of the SA24 sample, on unheated and heated up to 600°C specimens of the PK4 sample and on unheated and heated up to 640°C specimens of the A30 sample.

Room temperature ^{57}Fe Mössbauer spectra were taken on unheated and heated up to 600°C specimens of the BR48 sample, in a 512-channels constant-acceleration conventional spectrometer with a nominal 15mCi ^{57}CoRh source. The spectra were fitted to Lorentzian line-widths with a non-linear least-squares program. Isomer shifts are referred to an α-Fe foil at room temperature.

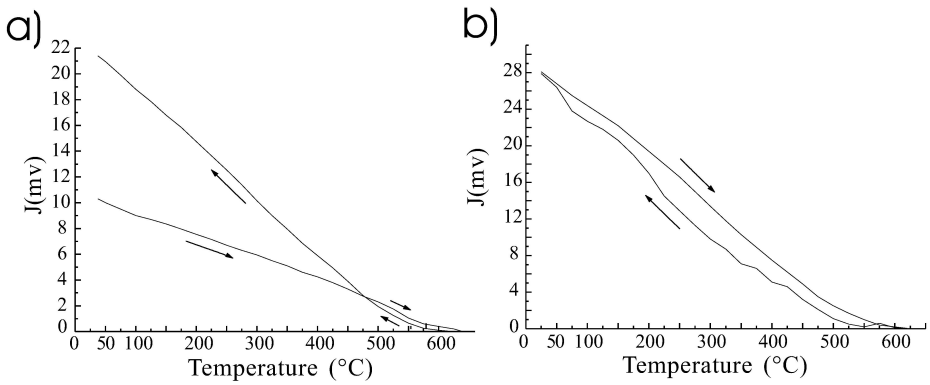

Fig. 3. Thermomagnetic curves. **a)** First run on specimen BR48; **b)** Second run on the same specimen.

4. RESULTS

4.1. Magnetic measurements

Two successive thermomagnetic curves were performed on the same BR48 specimen in air atmosphere. The intensity of the applied field was 0.5 T. A heating/cooling rate of 10°C/minute was used. In the first run, the magnetization decreased evenly with increasing temperature. On cooling below the Curie point (of approximately 580°C) a strong magnetization increased smoothly and continuously down to room temperature (Fig. 3a). Clearly a ferromagnetic mineral is created in the thermal treatment. The second thermomagnetic curve carried out on the same specimen is reversible (Fig. 3b). These curves show that all the new ferromagnetic mineral is formed in the course of the first heating/cooling cycle.

Bulk magnetic susceptibility (κ) vs. temperature (T) curves (Fig. 4) are irreversible, κ values at room temperature after cooling are remarkably higher than the initial values, indicating that a new ferrimagnetic mineral phase was created during thermal treatment.

IRM acquisition and back field experiments were conducted on the natural and their respectivelly thermally demagnetized specimens after different heating steps (600, 620, 640, 660, 700 and 730°C) (Fig. 5) (Table 1). It can be observed that a ferrimagnetic mineral with low coercive force (magnetite and/or maghemite) was generated during the incremental heating at 620°C, 660°C and in some cases at 730°C (Fig. 5). However, when the A samples are heated up to 730°C a remarkable decrease in the content of ferrimagnetic minerals of low-coercive force, simultaneously with the generation of antiferromagnetic minerals of high-coercive force is observed. In order to analyze in more detail the coercivity spectra derived from the IRM curves, the incremental isothermal remanent moments (ΔJ Am^2/kg) in 100 mT intervals were calculated for unheated and heated specimens of the same sample, and plotted as histograms (*Dunlop, 1972*). It can be

observed that in all cases the most important changes occurred in the 100 mT coercivity fraction. Heating in air up to 600, 620, 640, 660 and in some cases 730°C resulted in the production of magnetite and/or maghemite (Fig. 6). The other coercivity fractions underwent minor modifications (Fig. 6). This fact would suggest that the magnetite and/or maghemite was formed through the transformation of non ferromagnetic minerals. In the case of some A samples, the new magnetite and/or maghemite disappeared after heating in air at 730°C (Fig. 6). At the same time, the generation of some hematite would have occurred (see 700–1000 mT coercivity fractions in A53 and A32 samples in Fig. 6). The above mentioned transformations (production of magnetite and/or maghemite after 600–660°C heating and its disappearance in A samples after 730°C heating simultaneously with the additional generation of hematite) are supported by the corresponding variation in H_{cr} and J_{rs} parameters (Table 1).

Hysteresis curves were obtained at room temperature on several samples before and after different heating steps (500, 600, 620, 640, 660, and 730°C) (Fig. 7). It was observed that after heating at 600–660°C, and in some cases at 730°C, the presence of a new ferrimagnetic mineral was detected. However, when subjected to demagnetization at 720–730°C a remarkable decrease in the content of ferrimagnetic minerals of low coercive force was registered in the case of the A samples (Fig. 7). To better determine the

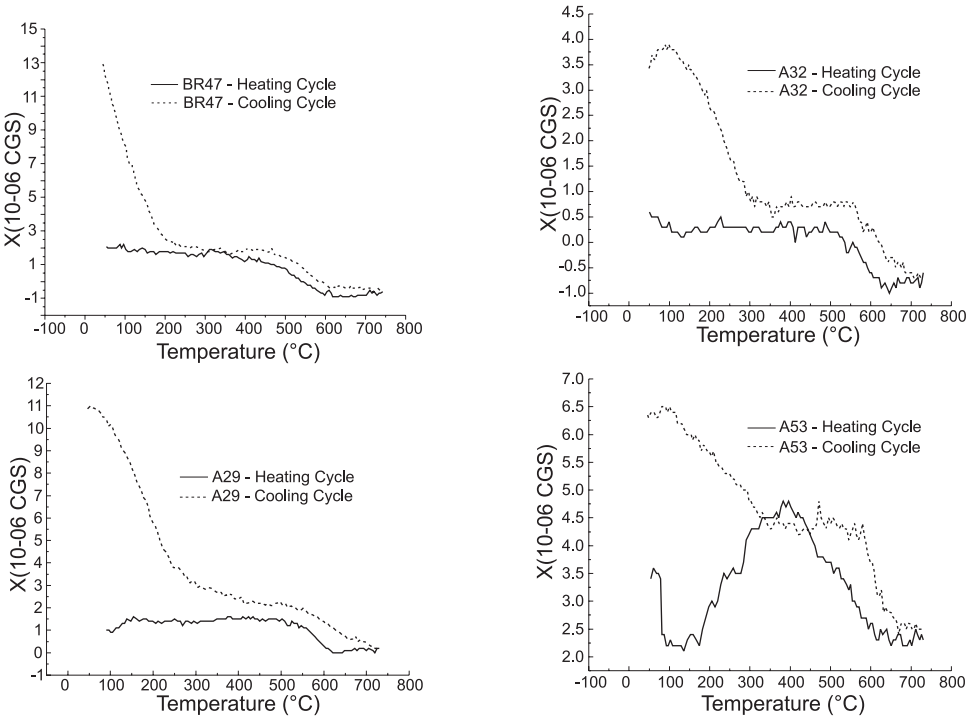

Fig. 4. Bulk magnetic susceptibility (κ) vs. temperature (T) curves.

characteristics of the mineralogical changes, curves of the difference of the hysteresis loops before and after heating were calculated (Fig. 8). In all cases the shape of the difference curves between the hysteresis loops of unheated and heated up to 600–660°C and in some cases 730°C specimens were simple, indicating the formation of new ferrimagnetic minerals of low coercive force (Fig. 8). When the hysteresis loops of A specimens heated up to 620°C were subtracted from the loops of A specimens heated up to 730°C, it could be determined that a ferrimagnetic phase disappeared (Fig. 8). These results coincide with the variations of the values of H_c and J_s calculated for each specimen

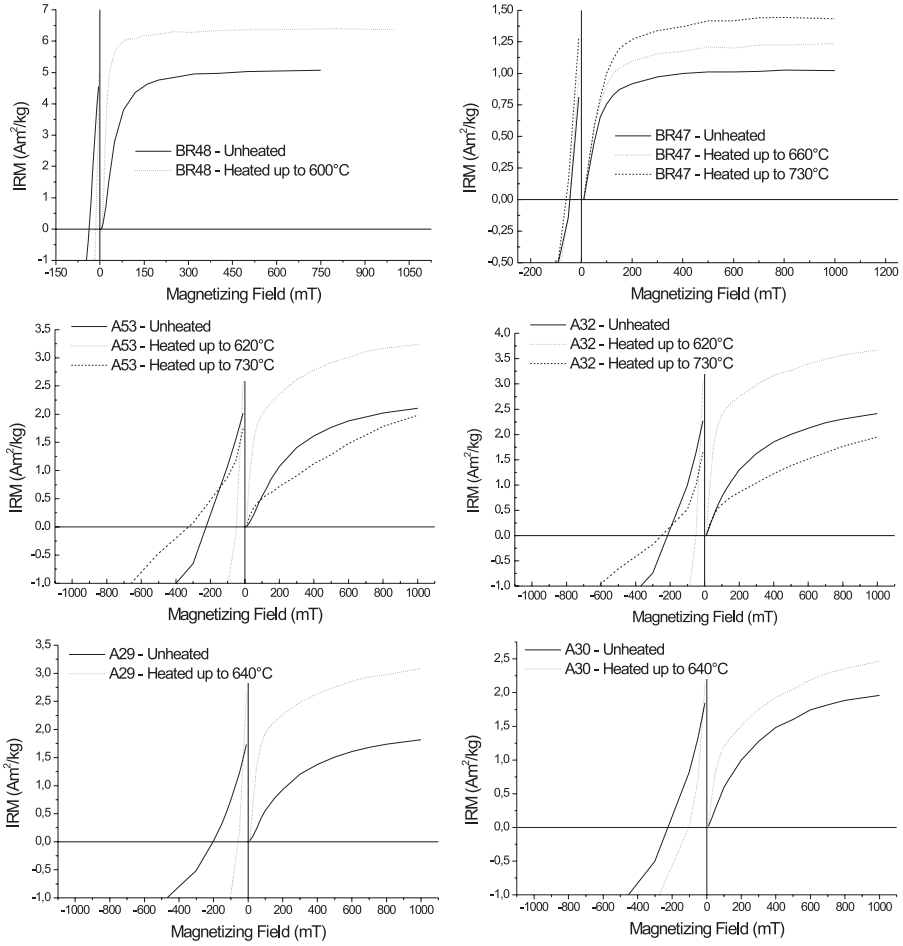

Fig. 5. IRM acquisition and back field curves conducted on natural and on the correspondent thermally demagnetized specimens.

Table 1. Values of main magnetic parameters at each temperature step for different samples. Values correspond to loops corrected of paramagnetic effect.($\%\kappa_{pa}$ - percentage of paramagnetic susceptibility, $\%\kappa_{fe}$ - percentage of ferromagnetic susceptibility).

Samples	J_s [Am^2/kg]	J_{rs} [Am^2/kg]	H_c [mT]	H_{cr} [mT]	$\%\kappa_{pa}$	$\%\kappa_{fe}$
BR47	6.8	1.5	13.6	45.9	21.8	78.2
BR47-660°C	11.5	1.7	5.9	45.9	12.1	87.9
BR47-730°C	28.2	1.9	3.5	60.33	6.1	93.9
BR48	27.5	4.2	12	38	8.7	91.3
BR48-600°C	41.5	5.5	5.3	16.5	1.5	98.5
SA24	0.7	0.7	49.2	414.5	59.3	40.7
SA24-700°C	3.3	0.9	15.4	322.6	33.6	66.4
PK4	2	1.4	146.3	466.1	62.8	37.2
PK4-600°C	12.3	2.2	6.4	279.8	12.2	87.8
PK5	0.9	1.1	251.6	443.5	76.1	23.9
PK5-600°C	6.9	1.8	15.2	305.8	36.6	63.4
A27	4.5	2.5	94.8	257.2	48	52
A27-640°C	9.8	2.9	17.6	227.9	20.2	79.8
A29	4.7	2.6	55.1	201.9	32.3	67.7
A29-640°C	17.2	4.2	15.1	59	7	93
A30	4.7	2.5	57.3	225.5	33.7	66.3
A30-640°C	12.8	3.2	15.3	102.7	9.6	90.4
A32	8.4	3.4	51.3	213.6	28.9	71.1
A32-620°C	21.9	5.3	13.9	48.2	7.3	92.7
A32-730°C	11.4	2.6	10.7	250.3	13.9	86.1
A53	5.1	3	106.9	227.5	50.3	49.7
A53-620°C	22.7	4.6	9.9	48.6	9.9	90.1
A53-730°C	10.2	2.7	13.1	324.8	22.7	77.3

(Table 1). It is important to note that some hysteresis cycles of red sandstone samples presented a marked "wasp-waist" after heating at 600–730°C (Fig. 7). In order to determine if this behavior was indicative of mixture of magnetite and/or maghemite and hematite, or alternatively attested the co-existence of SP-SD grains, we analyzed the hysteresis loops according to *Tauxe et al. (1996)*. We plotted the difference between the descending and ascending normalized loops (corrected of paramagnetic effect) for magnetizing fields > 0 mT. We termed such curves "ΔJ curves". The derivatives of the ΔJ curves for different samples are shown in Fig. 9. In these derivative curves one hump means one coercivity fraction in the loop. The existence of two distinct coercivity fractions was observed in all our samples (Fig. 9). A decrease of coercivity occurred after heating at 600–700°C, while a very important increase was registered after heating at 730°C (Fig. 9). These results are indicative of the generation of magnetite and/or maghemite when the samples were heated up to 600–700°C. Such magnetite and/or maghemite would disappear and hematite would form after heating at 730°C.

Moreover, in all cases a decrease of H_c, H_{cr} and the percentage of paramagnetic susceptibility ($\%\kappa_{pa}$) simultaneously with an increase of J_s, J_{rs} and the percentage of

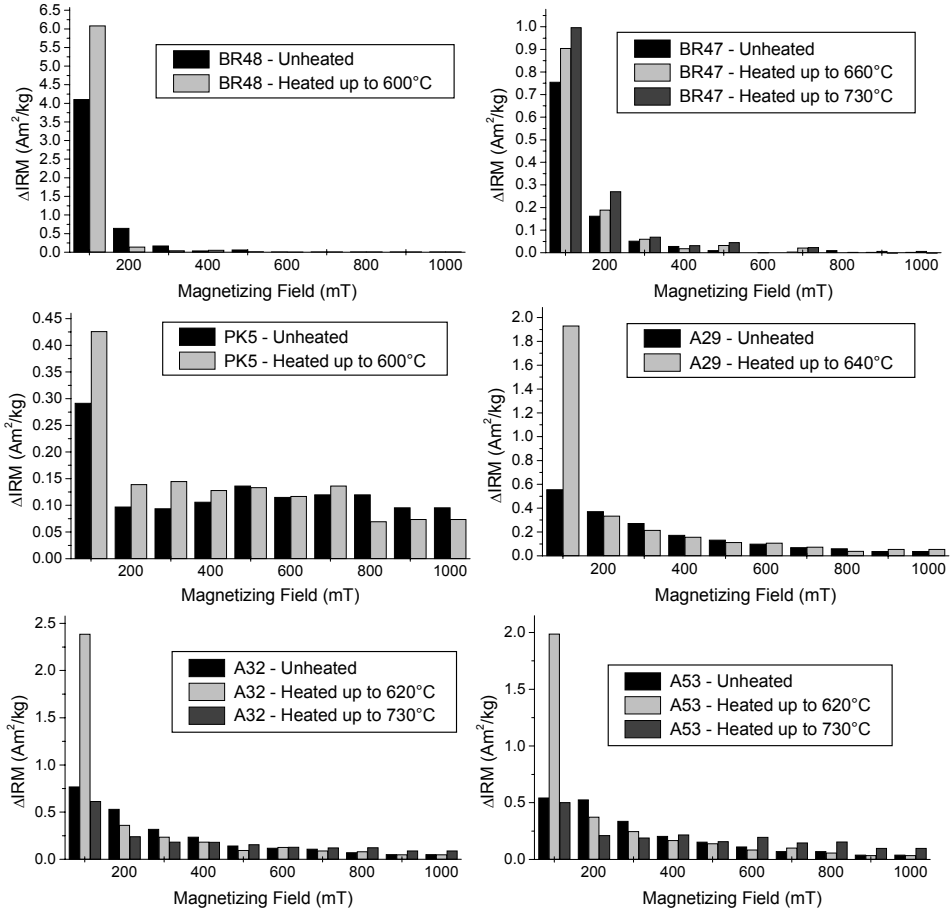

Fig. 6. Coercivity spectrum (plotted as histogram) of IRM acquisition curves for natural and the correspondent thermally demagnetized specimens.

ferromagnetic susceptibility (%κ_{fe}) was registered after heating at 600–700°C, suggesting the formation of magnetite and/or maghemite (Table 1). The A specimens heated up to 730°C show a remarkable increase of H_{cr} and %κ_{pa} and a decrease of J_s, J_{rs} and %κ_{fe}, suggesting the disappearance of magnetite and/or maghemite and the generation of hematite (Table 1).

4.2. XRD

X ray diffractometry analysis was carried out to determine compositional differences between heated and unheated specimens of BR48 sample. But only the presence of quartz, plagioclase, one or two micas, calcite and sulphates could be identified. For the heated sample, only changes in intensity of some peaks were observed, but very few peaks appeared or disappeared.

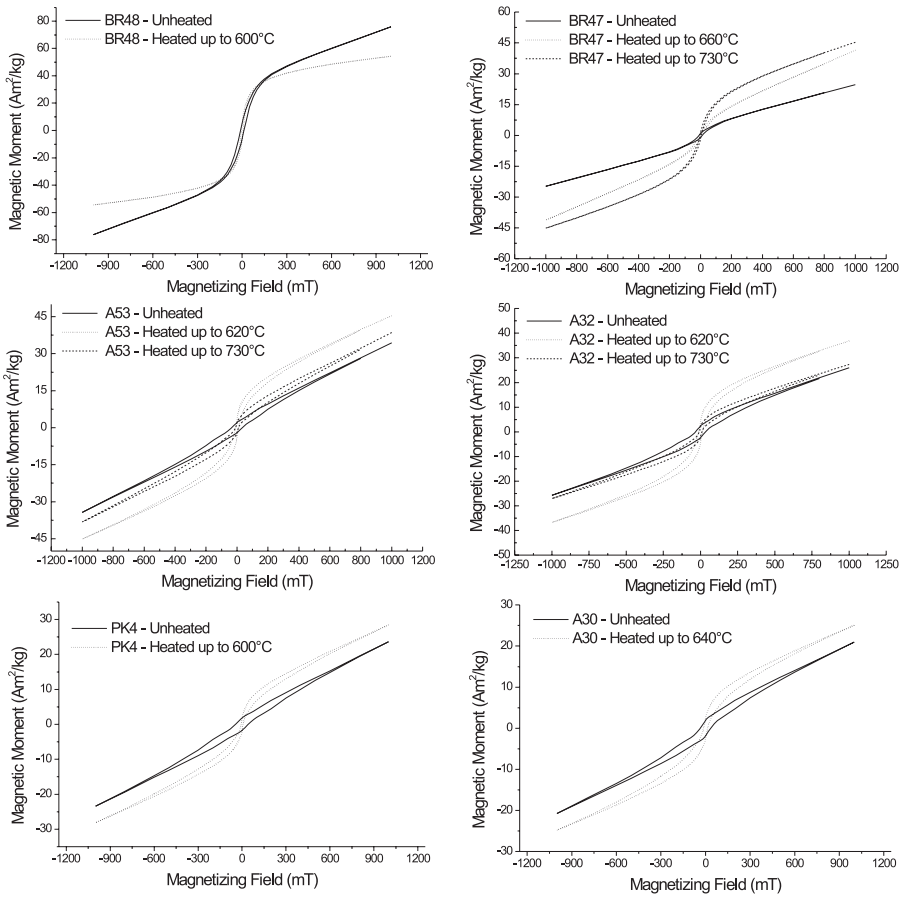

Fig. 7. Hysteresis curves conducted on natural and on the correspondent thermally demagnetized specimens.

4.3. Optical microscopy

Through the observation of thin sections of heated and unheated samples of green sandstones, it could be determined that the above mentioned change in color is due to transformations of the chloritic matrix. Upon heating the green chloritic matrix turns yellowish brown. In the unheated samples 2% of siderite of high refraction index in microcrystalline aggregates of nearly 200 μm in diameter were identified (Fig. 10a), these carbonates are absent in the correspondent heated samples. Likewise, in such heated samples numerous grains of ore minerals with irregular borders were observed which are not present in unheated samples. In the case of the red sandstones the presence of abundant calcite was determined in both heated and unheated specimens (Fig. 10b).

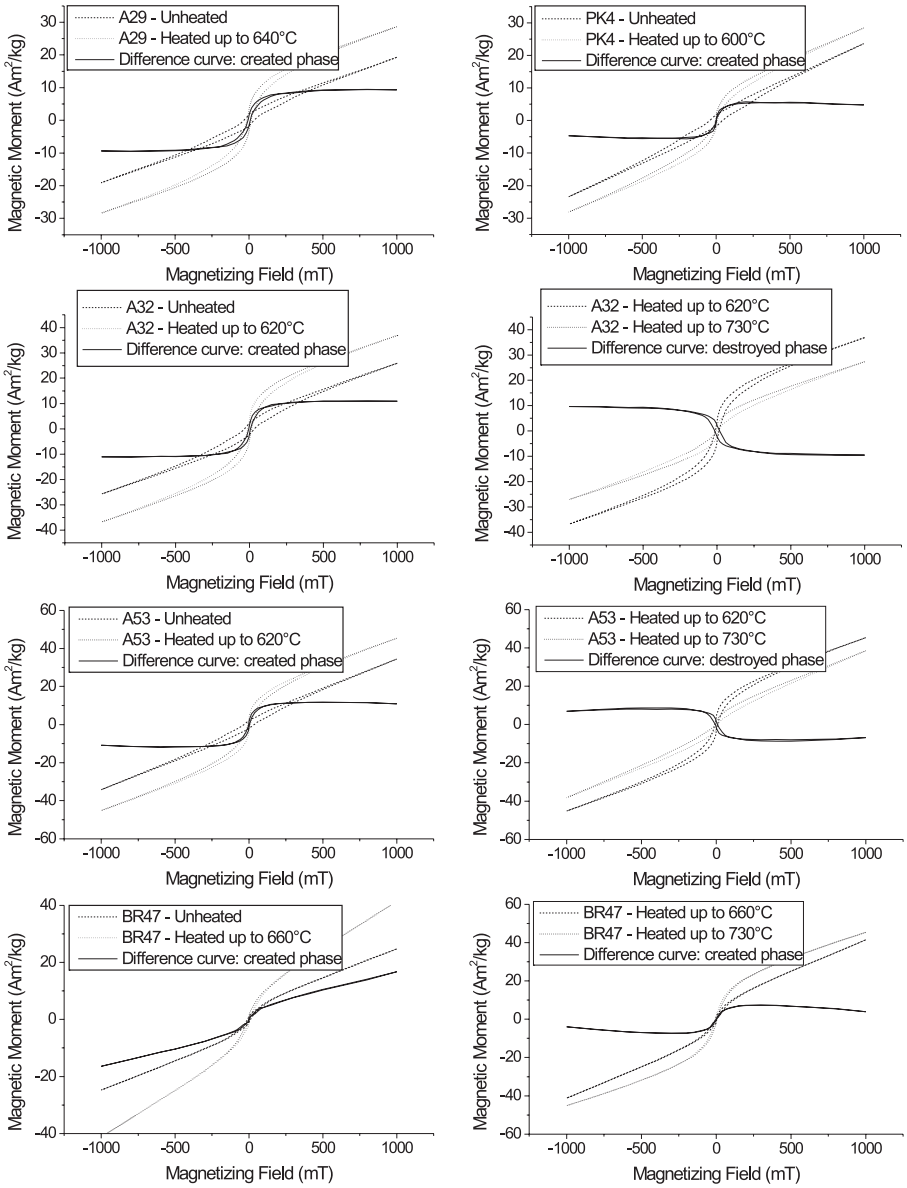

Fig. 8. Curves of hysteresis loops before and after heating for different samples, showing the generation or disappearance of magnetic phases during thermal treatment.

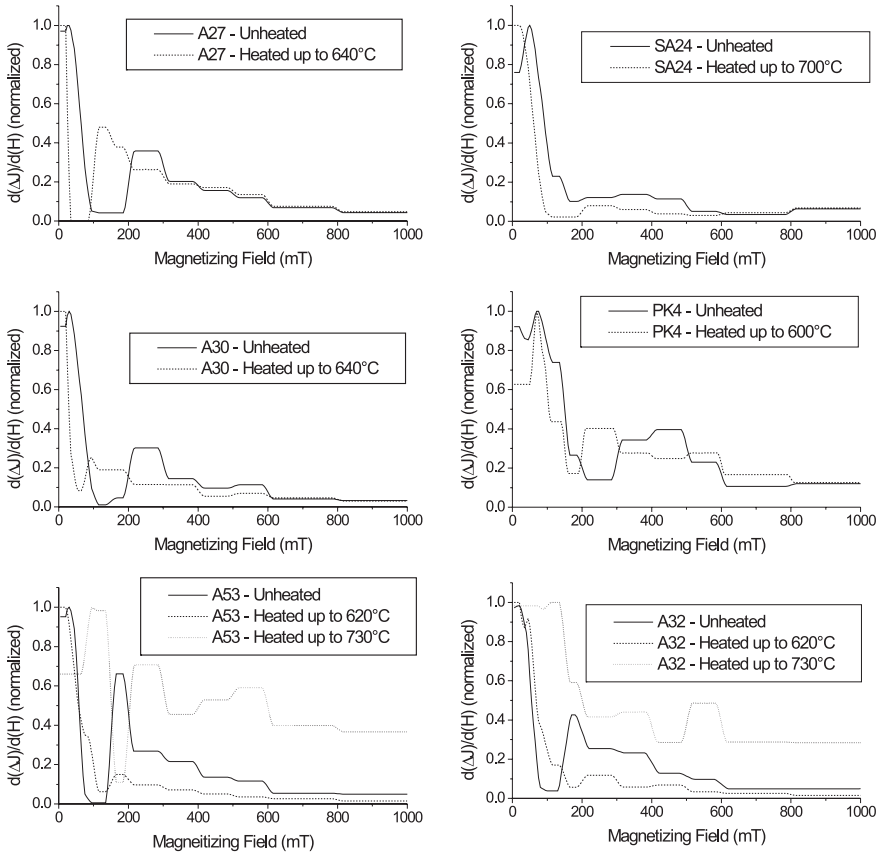

Fig. 9. Derivatives of the ΔJ curves of different red sandstone samples are shown for natural and the corresponding thermally demagnetized specimens.

Through the observation of polished sections of green sandstones heated samples the presence of numerous maghemite individuals of nearly 200–250 μm in diameter with very irregular edges was determined (Fig. 10c-f). Such maghemite would have been formed from the matrix or the cement of the rock. In the case of the unheated samples the presence of maghemite was not detected. No differences were distinguished between heated and unheated specimens of red sandstones. The new minerals generated during heating could have too small grain size to be observable.

4.4. Chemical analyses

The qualitative analyses of green sandstones specimens indicate the existence of siderite in the unheated sample and its absence in the heated one. The results of the

quantitative analyses showed an important decrease of ferrous oxide simultaneously with a notorious increase of ferric oxide contents after thermal treatment of green sandstones. Moreover, in the unheated sample the presence of carbon dioxide was determined, while in the heated one carbon dioxide was not detected (Table 2). In the case of the red sandstones, the heated specimens showed a higher content of ferric oxide than the unheated ones, but the contents of ferrous oxide and carbon dioxide did not exhibit significant changes (Table 2).

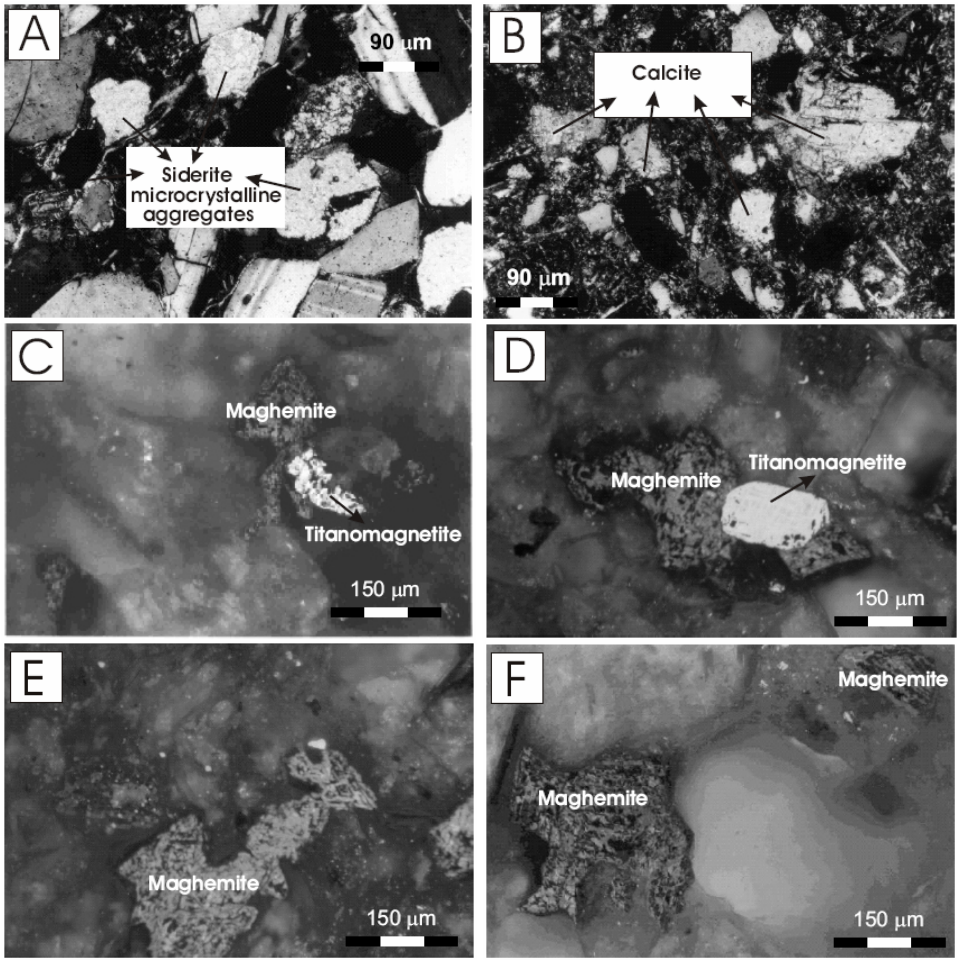

Fig. 10. Microphotographs of microscopy observation. **A:** thin section of a natural green sandstone specimen showing the presence of microcrystalline aggregates of siderite. **B:** thin section of a natural red sandstone specimen, where the existence of abundant calcite can be observed. **C, D, E** and **F:** polished section of a heated specimen of a green sandstone sample, showing the presence of maghemite and titanomagnetite.

Table 2. Quantitative chemical analysis carried out on heated and unheated specimens of green (BR48) and red (SA 24, PK4, A30) sandstones.

	Fe_2O_3	FeO	CO_2
BR48	1.89%	1.43%	detected
BR48 - 600°C	3.17%	0.38%	not detected
A30	4.98%	0.09%	3.80%
A30 - 640°C	5.00%	0.09%	3.90%
SA24	3.56%	0.23%	20.02%
SA24 - 700°C	4.40%	0.30%	18.10%
PK4	5.71%	0.10%	3.60%
PK4 - 600°C	5.83%	0.10%	4.33%

4.5. Mössbauer spectroscopy

The room temperature Mössbauer spectra of the unheated or heated BR48 green sandstone sample taken from –12 to +12 mm/s did not show any magnetically split signal within the statistical uncertainty. This is indicative that the iron oxides or oxihydroxides are made up of fine particles in a superparamagnetic regime, are in a very low amount or that room temperature is higher than the magnetic ordering temperatures of the iron species.

The spectrum taken from –3.5 to +3.5 mm/s (Fig. 11, Table 3) is made up of signals belonging to Fe^{3+} and Fe^{2+}. The area of the Fe^{3+} signal amounts to 58% of the spectrum and its parameters are characteristic of an octahedral coordination. The area of the Fe^{2+} signal comprises 41% of the spectrum and can be assigned to siderite. The spectrum of the green sandstone sample heated at 600°C contains 94% of Fe^{3+} and the spectral area of the Fe^{2+} signal has decreased to a maximum of 6%.

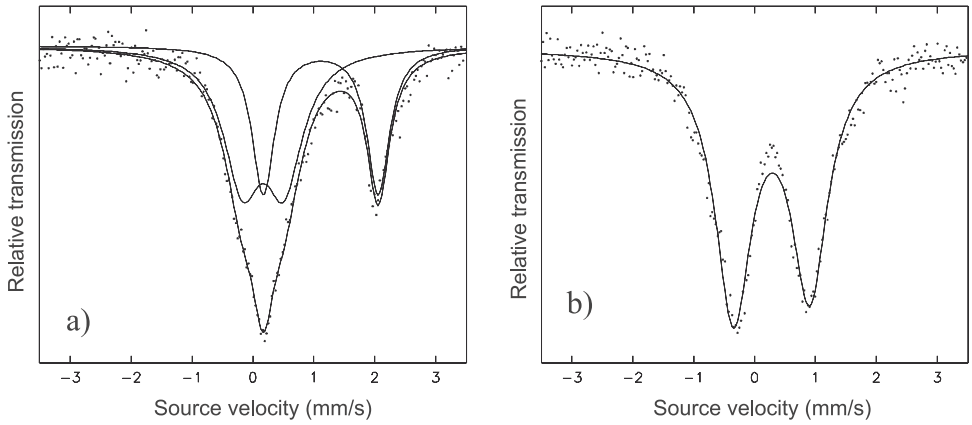

Fig. 11. Mössbauer spectra of BR48 sample: **a)** before, and **b)** after heating to 600°C.

Table 3. Hyperfine parameters of the BR48 green sandstone sample before and after heating.

Siderite					
	Delta [mm/s]	Delta [mm/s]			
	1.80	1.24			
BR48 Unheated					
	Delta [mm/s]	Delta [mm/s]	Gamma [mm/s]	%	Fe
1st Quadrupolar Interaction	0.68 ± 0.03	0.28 ± 0.02	0.74 ± 0.03	58 ± 6	3+
2nd Quadrupolar Interaction	1.89 ± 0.03	1.22 ± 0.02	0.45 ± 0.02	41 ± 5	2+
BR48 Heated to 600°C					
	Delta [mm/s]	Delta [mm/s]	Gamma [mm/s]	%	Fe
Quadrupolar Interaction	1.25 ± 0.03	0.39 ± 0.03	0.72 ± 0.02	100 ± 4	3+

5. DISCUSSION

Rowland and Jonas (1949) and *Kulp et al. (1951)* carried out differential thermal analysis, determining that pure siderite presented a unique endothermic peak with characteristic temperature of approximately 500°C and peak temperature of 585°C. Also, they could identify two variable exothermic peaks at 670°C and 830°C. The endothermic peak represents the decomposition of siderite to ferrous oxide. This is oxidized to maghemite giving the first major exothermic peak. The second exothermic peak is due to the transformation of maghemite to hematite. *Ellwood et al. (1986)* studied the magnetic properties of siderite-bearing limestones and determined that after sampling, air exposure, and oxidation in the laboratory, siderite generated intermediate chemically unstable maghemite or magnetite, which finally converted or oxidized to stable hematite. *Pan et al. (2000)* studied the oxidation products of high-purity crystalline siderite when thermally treated in air atmosphere. They determined that susceptibility increased sharply between 400 and 530°C, indicative of new ferrimagnetic mineral phase generation (magnetite). They observed that hematite is the terminal product if siderite is heated to 700°C and over. They concluded that magnetite, maghemite and hematite are the transformation products of high-temperature oxidation of siderite in air, and that maghemite was not completely inverted to hematite even at temperatures as high as 690°C during incremental thermal treatment. Considering the results we obtained, we hypothesize that the bulk magnetic susceptibility increases underwent by the studied sandstones samples during incremental heating would be explained by the generation of maghemite and/or magnetite from siderite, which is present in low amount as cement. In some cases (A samples) such maghemite and/or magnetite would invert to hematite at temperatures higher than 620°C.

The presence of iron oxides in the studied green sandstones could not be detected by XRD indicating that the percentage of these phases is below the detection sensitivity of the technique. Also the samples did not show any magnetically split signal at room temperature in their Mössbauer spectra. This is coherent with the XRD results and demonstrates the very small amount of iron oxides that the samples have in their composition. The possible contribution of any iron oxide (magnetite, maghemite or hematite) has to be found in the very broad central signal, which for simplicity was fitted with a Lorentzian line-shape. However, the magnetic response of the iron oxides is

≈40 times larger than any other mineral existing in the samples (*Fabris, 2002*). Thus the large magnetization changes observed in the samples has to be assigned to changes in the iron oxides.

The Mössbauer spectra (Fig. 11) display only broad quadrupole signals that may belong to several iron species with similar hyperfine parameters. Because the samples have a minor percentage of iron, the spectra had to be taken over many days to attain a reasonable statistics, in spite of the optimum choice of the absorber thickness used after the method described by *Rancourt et al. (1993)*. The hyperfine parameters of the unheated green sample belong to Fe^{2+} and Fe^{3+} species (Table 3). Although the broad lines are indicative of a high structural or chemical disorder, the Fe^{2+} parameters are close to those of siderite (δ = 1.24 mm/s, Δ = 1.80 mm/s). The other signal comprises Fe^{3+} ions that may belong to several iron minerals or to iron-substituted minerals and to superparamagnetic iron oxides. The heated green sample only contains a Fe^{3+} signal, which has been fitted to unreasonable broad Lorentzians, but because of the poor statistics, a fitting to a hyperfine distribution of parameters would also yield results with high statistical uncertainty.

The presence of siderite in the unheated green specimens and its absence in the heated ones was confirmed through the observation of thin sections and through qualitative and quantitative chemical analyses (Table 2).

Through the observation of the polished sections of green sandstones heated samples, the presence of maghemite (200–250 μm in diameter), which formed from the matrix or the cement of the rock during thermal demagnetization, was determined. In the case of the unheated samples the presence of maghemite was not detected. The size of such maghemite is large, but it could correspond to microcrystalline aggregates formed through the oxidation of the siderite microcrystalline aggregates (200 μm in diameter) identified in the thin sections of the unheated green sandstones.

The magnetic measurements clearly showed the generation of maghemite and/or magnetite in the samples heated up to 600–700°C (Table 1). In the case of the red sandstones such maghemite and/or magnetite disappeared when the samples were heated up to 730°C, simultaneously with the formation of hematite (Table 1). These mineralogical transformations support our hypothesis. However it is important to mention, that the presence of siderite in the unheated red sandstones could not be unequivocally established. The observation of thin sections revealed the existence of abundant carbonates in the heated and unheated samples. The new minerals generated during heating could not be observed in the polished sections. They would have too small grain size to be observable. The chemical analyses (Table 2) did not provide unambiguous evidences about the existence of siderite in unheated specimens. The presence of carbonates (CO_2 content) is detected in heated and unheated specimens (Table 2). Only in the case of SA24 sample the content of carbon dioxide decreased after heating (Table 2). These samples contain abundant calcite, which possesses decomposition temperatures > 900°C (*Kulp et al., 1951*), and can present substitution of Ca^{2+} by Fe^{2+}. This last fact could explain the results of the chemical analyses.

In the case of the red sandstones only the magnetic measurements were able to detect the mineralogical changes occurred during heating. However, the temperatures at which such changes take place (susceptibility increases after 570°C, maghemite and/or magnetite forms between 570–600°C, such maghemite and/or magnetite inverts to hematite between

640–730°C), would suggest the existence of siderite in the studied samples. Perhaps low temperature experiments (*Pan et al., 2002*; *Frederichs et al., 2003*) could help to confirm the presence of siderite in the unheated samples, revealing its transition at 35–40 K. Nevertheless, it is important to mention that *Pan et al. (2002)* and *Frederichs et al. (2003)* used samples containing approximately 95% and 100 % siderite for their experiments, respectively. In our samples siderite would be present in very minor amounts. This fact could hinder the identification of siderite through low temperature magnetic measurements.

In order to further support our hypothesis, it is important to mention that in the depositional and diagenetic environments of the red and green sandstones studied here, the formation of authigenic siderite is very common. In volcaniclastic sandstones (like the ones studied here) iron rich chlorites are normally generated during the early diagenesis. *Weaver (1989)* proposed that at about 160°C and with high contribution of iron and magnesium of volcanic origin, ferrous chlorites are generated which confers green color to the sandstones. *Larsen and Chilingar (1967)* mentioned that a usual paragenetic association of diagenetic minerals is the one formed by: siderite, chlorite and calcite. *Dapples (1967)* proposed that in a slightly reducing environment, with presence and precipitation of calcite and siderite (pH ~ 8), chlorite would be generated from biotite giving green color to the sedimentary rocks. This reducing environment is very common immediately after the deposition during early diagenesis at temperatures < 100°C (*Dapples, 1967*). A similar reaction is postulated by *Turner (1980)*, he proposed that during diagenesis in a reducing environment ferrous iron rich chlorites would form from hornblende, producing green zones in the sedimentary rocks. This reducing environment could be due to the presence of underground waters saturated in electrolytes.

The formation of red beds during burial diagenesis was clearly described by *Walker (1967)* and *Walker et al. (1978)*. The key to this mechanism is the intrastratal alteration of ferromagnesian silicates by oxygenated groundwaters during burial. A feature of this process is the production of a suite of by-products which are precipitated as authigenic phases. These include mixed layer clays (illite-montmorillonite), quartz, potash feldspars and carbonates as well as the pigmentary ferric oxides. *Dapples (1967)* proposed that in an oxidizing environment hematite and caolinite and/or illite would be generated from biotite, giving red coloration to sedimentary rocks. *Turner (1980)* suggested that in an oxidizing environment hematite would form from hornblende conferring red color to the rocks. Nevertheless, these authors postulated that very local conditions of oxidation-reduction can exist that would generate leached sectors in the red beds. *Dapples (1967)* indicated that there could be zones saturated in water with high content of electrolytes, with high pH that would produce the substitution of clays by calcite, dolomite and siderite in the red beds. *Turner (1980)* mentioned that reducing and oxidizing environments can occur successively along time during digenesis. If we consider that the sandstones studied here correspond to sedimentary sections with interlayered ignimbrites and/or tuffs and with considerable volcaniclastic contribution, reduction would probably superimpose oxidation due to the circulation of water rich in electrolytes coming from the volcanic material. Therefore, in such environments the presence of siderite as cement would be quite common, explaining the bulk magnetic susceptibility increases registered during thermal demagnetization of the continental red and green sandstones studied here.

The mineralogical changes occurred during laboratory routines are interesting, because they can be controlled and can help to understand natural processes. This is particularly important in the case of magnetizations carried by hematitic pigment in red beds. The generation of secondary hematite would produce a magnetic phase that could dominate the magnetization of samples whose content of iron oxides were initially low.

Further work is necessary in order to completely understand the mineralogical changes suffered by continental sandstones when submitted to thermal demagnetization.

6. CONCLUSIONS

1. Siderite, which is present in the studied samples as cement in low quantities, was addressed as the main cause of the rise in the bulk magnetic susceptibility underwent by the green continental natural sandstones when thermally treated.
2. We suggest that siderite would also be responsible of the bulk magnetic susceptibility increases suffered by the red continental natural sandstones during high temperature demagnetization.
3. Such susceptibility increases would be due to magnetite and/or maghemite generation from siderite oxidation. The subsequent inversion to hematite was also observed in some red sandstones.
4. Futher work is needed in order to fully understand the mineralogical changes underwent by continental sandstones during thermal treatment.

Acknowledgements: We wish to thank specially Drs. Milka Brodtkorv and Renato Andreis for their careful observation of thin and polished sections of green and red sandstones samples of Tiomayo and Pozuelos Formation. C. Prezzi gratefully acknowledges the support of an Alexander von Humboldt Research Fellowship from the Alexander von Humboldt Foundation, during which this paper was finished. Most of the IRM, back field, hysteresis and k vs. T curves were measured at the paleomagnetism laboratory of the Instituto Astronômico e Geofisico, Universidade de São Paulo, Brazil as part of the Scientific-Technologic Cooperation Project with Brazil BR21/00.

References

Coira B., Caffe P., Ramirez A., Chayle W., Rosas S., Diaz A., Perez B., Orosco O. and Martinez M., 2005. *Hoja Geológica 2366-I Mina Pirquitas*. Dirección Nacional del Servicio Geológico, Buenos Aires, Argentina (in press).

Dapples E., 1967. Diagenesis of Sandstones. In: G. Larsen and G. Chilingar (Eds.), *Diagenesis in Sediments*. *Developments in Sedimentology*, **8**, Elsevier Scientific Publishing Company, Amsterdam.

Dunlop D., 1972. Magnetic Mineralogy of Unheated and Heated Red Sediments by Coercivity Spectrum Analysis. *Geophys. J. R. Astron. Soc.*, **27**, 37–55.

Ellwood B., Balsam W. and Burkart B., 1986. Anomalous Magnetic Properties in Rocks Containing the Mineral Siderite: Paleomagnetic Implications. *J. Geophys. Res.*, **91(B12)**, 12,779–12,790.

Fabris J.D. and Coey J.M.D., 2002. Espectroscopia Mössbauer do ^{57}Fe e Medidas Magnéticas na Análise de Geomateriais. *Tópicos em Ciência do Solo*, **2**, 47-102, Sociedade Brasileira de Ciência do Solo, Viçosa, Brasil.

Frederichs T., von Dobeneck T., Bleil U. and Dekkers M., 2003. Towards the Identification of Siderite, Rhodochrosite, and Vivianite in Sediments by Their Low Temperature Magnetic Properties. *Phys. Chem. Earth*, **28**, 669–679.

Haggerty S., 1991. Oxide Textures - a Mini Atlas. In: D. Lindsley (Ed.), *Oxide Minerals: Petrologic and Magnetic Significance. Reviews in Mineralogy*, **25**, 129–219.

Isambert A., Valet J.P., Gloter A. and Guyot F. 2003. Stable Mn-Magnetite Derived from Mn-Siderite by Heating in Air. *J. Geophys. Res.*, **108**, doi: 10.1029/2002JB002099.

Kulp J., Kent P. and Kerr P., 1951. Thermal Study of the Ca-Mg-Fe Carbonate Minerals. *Am. Miner.*, **36**, 643–670.

Larsen G. and Chilingar G., 1967. Diagenesis in Sediments and Sedimentary Rocks. In: G. Larsen and G. Chilingar (Eds.), *Diagenesis in Sediments*. *Developments in Sedimentology*, **8**, Elsevier Scientific Publishing Company, Amsterdam.

Pan Y., Zhu R. and Banerjee S., 2000. Rock Magnetic Properties Related to Thermal Treatment of Siderite: Behavior and Interpretation. *J. Geophys. Res.*, **105(B1)**, 783–794.

Pan Y., Zhu R., Liu Q. and Jackson M., 2002. Low-Temperature Magnetic Behaviour Related to Thermal Alteration of Siderite. *Geophys. Res. Lett.*, **29**, doi: 10.1029/2002GL016021.

Prezzi C., 1999. *Evolución Geodinámica de la Puna sobre la base de estudios paleomagnéticos*. Ph.D. Thesis, Buenos Aires University, Buenos Aires, Argentina.

Prezzi C. and Vilas J., 1998. New Evidence of Clockwise Vertical Axis Rotations South of the Arica Elbow (Argentine Puna). *Tectonophysics*, **292**, 85–100.

Prezzi C. and Alonso R., 2002. New Paleomagnetic Data from the Northern Argentine Puna: Central Andes Rotation Pattern Reanalyzed. *J. Geophys. Res.*, **107**, doi: 10.1029/2001JB000225.

Prezzi C., Caffe P. and Somoza R., 2004. New Paleomagnetic Data from the Northern Puna and Western Cordillera Oriental, Argentina: a New Insight on the Timing of Rotational Deformation. *J. Geodyn.*, **38**, 93–115.

Rancourt D.G., McDonald A.M., Lalonde A.E. and Ping J.Y., 1993. Mössbauer Absorber Thicknesses for Accurate Site Populations in Fe-Bearing Minerals. *Am. Miner.*, **78**, 1–7.

Rowland R. and Jonas E., 1949. Variations in Differential Thermal Analysis Curves of Siderite. *Am. Miner.*, **34**, 550–558.

Schwarz E.J., 1970. Magnetochemical Aspects of the Heating of Red and Green Beds. Paper 70-63, Geological Survey of Canada, 31–34.

Seggiaro R.E. and Aniel B., 1989. Los ciclos piroclásticos del área Tiomayo - Coranzulí, Provincia de Jujuy. *Revista de la Asociación Geológica Argentina*, **44**, 394–401.

Stephenson A., 1967. The Effect of Heat Treatment on the Magnetic Properties of the Old Red Sandstone. *Geophys. J. R. Astron. Soc.*, **13**, 425–440.

Tauxe L., Mullender T. and Pick T., 1996. Potbellies, Wasp-Waists, and Superparamagnetism in Magnetic Hysteresis. *J. Geophys. Res.,* **101(B1)**, 571–583.

Turner P., 1980. Continental Red Beds. *Developments in Sedimentology*, **29**. Elsevier Scientific Publishing Company, Amsterdam.

Vandervoort D., 1993. Non-Marine Evaporite Basin Studies, Southern Puna Plateau, Central Andes. Ph.D. Thesis. Cornell University, U.S.A.

Walker T.R., 1967. Formation of Red Beds in Modern and Ancient Deserts. *Bull. Geol. Soc. Amer.,* **78**, 353–368.

Walker T.R., Waugh B. and Crone A.J, 1978. Diagenesis in First Cycle Desert Alluvium of Cenozoic Age, Southwestern United States and Northwestern Mexico. *Bull. Geol. Soc. Amer.,* **89**, 19–32

Weaver C., 1989. Clays, Muds and Shales. *Developments in Sedimentology*, **44**, Elsevier Scientific Publishing Company, Amsterdam.